Journal of Geodesy (2003) 77: 217–225
DOI 10.1007/s00190-003-0313-x

Journal of Geodesy

A study on the combination of satellite, airborne, and terrestrial gravity data

M. Kern, K. P. Schwarz, N. Sneeuw

Department of Geomatics Engineering, The University of Calgary, 2500 University Drive NW, Calgary, Canada T2N 1N4
e-mail: mkern@ucalgary.ca; Tel.: +1 403 220 8794; Fax: +1 403 284 1980

Received: 5 June 2002 / Accepted: 20 December 2002

Abstract. Satellite gravity missions, such as CHAMP, GRACE and GOCE, and airborne gravity campaigns in areas without ground gravity will enhance the present knowledge of the Earth's gravity field. Combining the new gravity information with the existing marine and ground gravity anomalies is a major task for which the mathematical tools have to be developed. In one way or another they will be based on the spectral information available for gravity data and noise. The integration of the additional gravity information from satellite and airborne campaigns with existing data has not been studied in sufficient detail and a number of open questions remain. A strategy for the combination of satellite, airborne and ground measurements is presented. It is based on ideas independently introduced by Sjöberg and Wenzel in the early 1980s and has been modified by using a quasi-deterministic approach for the determination of the weighting functions. In addition, the original approach of Sjöberg and Wenzel is extended to more than two measurement types, combining the Meissl scheme with the least-squares spectral combination. Satellite (or geopotential) harmonics, ground gravity anomalies and airborne gravity disturbances are used as measurement types, but other combinations are possible. Different error characteristics and measurement-type combinations and their impact on the final solution are studied. Using simulated data, the results show a geoid accuracy in the centimeter range for a local test area.

Keywords: Least-squares spectral combination – Quasi-deterministic weight determination – Gravity field determination

Correspondence to: M. Kern

1 Introduction

One of the challenges in gravity field modeling in the near future will be the combination of different types of gravity measurement. Clearly, with the data from dedicated satellites such as CHAMP, GRACE and GOCE being available, additional information about the gravity field can be obtained. It will refine the present knowledge of the gravity field and make the existing low-frequency information more reliable. However, this new information is band limited and existing data sets such as ground gravity anomalies and airborne gravity data have to be used to recover the high frequencies of the gravity spectrum. Although most of the power of geoidal undulations is contained in the lower frequencies, absolute geoid determination in the centimeter range is not possible without combining all available gravity data.

An overview of methods that have been numerically investigated for combining satellite (or geopotential) models and terrestrial gravity anomalies is given in Pishchukhina (1987) or Featherstone et al. (1998). These methods use the satellite-derived geoidal undulations as the low-frequency part of the geoid and the residual terrestrial gravity anomalies as the medium- and high-frequency part of the geoid, applying a (modified) Stokes integration in the process. The weighting of the two measurement types is done with *deterministic* or *stochastic* approaches, (see Heck and Grüninger 1987). The deterministic methods neglect all possible stochastic a priori information about the data, sources and might in some cases be too pessimistic, whereas the stochastic solutions more or less rely on the quality of the error and noise estimates.

Less attention has been given to the combination of more than two measurement types. This is mainly due to the fact that acquiring gravity is expensive and multiple or redundant gravity campaigns are avoided. In some cases, however, and especially with the advent of airborne

gravimetry and gravity satellite missions, more (independent) gravity data sources over limited areas will be available. One possible strategy to combine multiple gravity measurement types is to solve the inherent overdetermined boundary-value problems (see e.g. Sacerdote and Sansò 1985; Keller 1991). In this model approach, the solutions are given for continuous gravity information all over the Earth. In this paper, the operational situation is taken into account. The individual measurement types may not only be different in spatial distribution, data type and stochastic properties, but can also differ considerably in their spectral characteristics (Schwarz 1984). This seems somewhat difficult to model in a boundary-value approach.

In the following, it is assumed that calibrated satellite data are available in spherical harmonics. Thus, a combination on the observation level is not considered. The classical combination approach is least-squares (LS) collocation (see Krarup 1969; Moritz 1989). Alternative methods are given with the multiple-input/single-output approach (Vassiliou 1986; Sideris 1996) and LS spectral combination (Sjöberg 1981; Wenzel 1981; van Gelderen-Rummel 2001).

This paper focuses on the LS spectral combination and has the following three objectives.

1. To develop a framework for band-limited integral combination methods;
2. To propose a quasi-deterministic approach for the determination of the weights that neither imposes assumptions on the data noise nor requires the a priori knowledge of the errors in the local or regional gravity data;
3. To assess the accuracy of the method using multiple data sets and different combinations.

2 A framework for band-limited integral combination methods

The framework for integral combinations described in this paper merges several concepts.

1. The discrete and band-limited formulation (Bjerhammar 1973).
2. The Meissl scheme (Meissl 1971; Rummel and van-Gelderen 1995).
3. The spectral combination (see e.g. Sjöberg 1981; Wenzel 1981; van Gelderen and Rummel 2001).

Truncation errors and other practical problems can generally be treated. Spherical approximation is used throughout the paper.

The functional model is given as (Rummel and van Gelderen 1995)

$$f = \frac{1}{4\pi} \iint_{\sigma} gK \mathrm{d}\sigma \tag{1}$$

where f are the output functionals and g stands for the input functionals. When the input functionals are limited in a frequency band from degree 2 up to the maximum (resolution) degree L, the respective kernel functions K become *band limited*. High-frequency noise may leak into the solution when full kernel functions are used. Hence, the (isotropic) kernel functions are given as

$$K = \sum_{\ell=2}^{L} (2\ell+1)\lambda_\ell P_\ell(\cos\psi) \tag{2}$$

where $P_\ell(\cos\psi)$ are the Legendre functions as defined in Heiskanen and Moritz (1967). Some of the most common eigenvalues λ_ℓ are summarized in Table 1. They can all be taken from the Meissl scheme (Rummel and van Gelderen 1995). R is the reference sphere radius and $r = R + H$ stands for the radius of a sphere at height H. Transformation of airborne gravity disturbances into the potential in one step was first used in Novák and Heck (2002). Although some of the kernel functions are divergent, the accuracy of the band-limited solutions is not adversely affected for most applications. Note that for some of the functionals the summation starts with a value other than two.

Residual gravity values are usually preferred in the integration process. The (high-frequency) residuals are obtained by subtracting the low-frequency satellite information from the original data g. They yield

$$\begin{aligned} g^{\mathrm{l}} &= g - g_{\mathrm{l}} \\ &= g - \frac{GM}{R} \sum_{\ell=2}^{L_{\mathrm{S}}} \kappa_\ell T_\ell \end{aligned} \tag{3}$$

where GM is the product of the Newtonian gravitational constant and the mass of the Earth, $L_{\mathrm{S}} < L$ is the maximum degree of the (satellite) spherical harmonics and T_ℓ are the (Laplace) surface spherical harmonics of the disturbing potential T. Table 2 shows selected values for κ_ℓ.

Table 1. Eigenvalues λ_ℓ

f	g	λ_ℓ	Name
$T(R)$	$\Delta g(R)$	$\frac{R}{\ell-1}$	Stokes
$T(R)$	$\delta g(R)$	$\frac{R}{\ell+1}$	Hotine
$T(R)$	$\Delta g(r)$	$\frac{r}{\ell-1}\left(\frac{r}{R}\right)^{\ell+1}$	One-step
$T(R)$	$\delta g(r)$	$\frac{r}{\ell+1}\left(\frac{r}{R}\right)^{\ell+1}$	One-step
$T(R)$	$T_{rr}(r)$	$\frac{r^2}{(\ell+1)(\ell+2)}\left(\frac{r}{R}\right)^{\ell+1}$	Gradiometry
$T(r)$	$T(R)$	$\left(\frac{R}{r}\right)^{\ell+1}$	Poisson

Table 2. κ_ℓ values

Functional	κ_ℓ
$\Delta g(r)$	$\frac{\ell-1}{r}\left(\frac{R}{r}\right)^{\ell+1}$
$\delta g(r)$	$\frac{\ell+1}{r}\left(\frac{R}{r}\right)^{\ell+1}$
$T(r)$	$\left(\frac{R}{r}\right)^{\ell+1}$
$T_{rr}(r)$	$\frac{(\ell+1)(\ell+2)}{r^2}\left(\frac{R}{r}\right)^{\ell+1}$

The frequency division of Eq. (1) yields

$$f = \frac{1}{4\pi}\iint_{\sigma} g^{\mathrm{l}} K \mathrm{d}\sigma + f_{\mathrm{l}} \tag{4}$$

where f_{l} is added to account for the low-frequency part. It is computed from the satellite data as

$$f_{\mathrm{l}} = \frac{GM}{R}\sum_{\ell=2}^{L_{\mathrm{S}}} \kappa_\ell T_\ell \tag{5}$$

The above integral methods are developed for continuously given input functionals g. In practice, however, the global and continuous integrals are replaced by discrete, area-limited summations due to the character of the available data. Thus, a spatial division of Eq. (4) has to be performed in addition to the frequency division. The corresponding equations may be derived using a simple window function w. The window equals 1 for the local data area and 0 for the rest of the integration domain σ. In this case, Eq. (4) becomes

$$\begin{aligned} f_f &= \frac{1}{4\pi}\iint w g^{\mathrm{l}} K \mathrm{d}\sigma + f_{\mathrm{l}} \\ &= \frac{1}{4\pi}\iint_{\sigma_0} g^{\mathrm{l}} K \mathrm{d}\sigma \ + f_{\mathrm{l}} \end{aligned} \tag{6}$$

σ_0 stands for the local data domain. However, discontinuities due to the sharp window function may occur and a truncation error exists due to the neglect of the distant zones.

The rest of the integration domain $\sigma - \sigma_0$ is accounted for in Molodensky's approach (Molodenskij 1958). The two integration parts are then referred to as *near-zone contribution* (σ_0) and *far-zone contribution* $(\sigma - \sigma_0)$ (see e.g. Vaníček Kleusberg 1987). Equation (4) is rewritten as

$$\begin{aligned} f &= f_{\sigma_0} + f_{\sigma-\sigma_0} + f_{\mathrm{l}} \\ &= \frac{1}{4\pi}\iint_{\sigma_0} g^{\mathrm{l}} K \mathrm{d}\sigma + \frac{1}{4\pi}\iint_{\sigma-\sigma_0} g^{\mathrm{l}} K \mathrm{d}\sigma + f_{\mathrm{l}} \end{aligned} \tag{7}$$

The far-zone contribution can be analytically computed, implying that the low-frequency part is removed up to degree $\ell = L_{\mathrm{S}}$ ($L_{\mathrm{S}} \approx 300$ for GOCE) and that the missing gravity data can be estimated from a geopotential model ($L_{\mathrm{M}} = 360$ for EGM96) as

$$g^{\mathrm{l}} \approx g^{\mathrm{M}} = \frac{GM}{R}\sum_{\ell=L_{\mathrm{S}}+1}^{L_{\mathrm{M}}} \kappa_\ell T_\ell^{\mathrm{M}}, \qquad L_{\mathrm{S}} \le L_{\mathrm{M}} \tag{8}$$

where T_ℓ^{M} are (Laplace) surface spherical harmonics from the geopotential model. Inserting Eq. (8) and the kernel function into the second integral of Eq. (7) leads to the far-zone contribution

$$\begin{aligned} f_{\sigma-\sigma_0} &= \frac{1}{4\pi}\iint_{\sigma-\sigma_0} g^{\mathrm{l}} K \mathrm{d}\sigma \\ &\approx \frac{GM}{2R}\sum_{\ell=L_{\mathrm{S}}+1}^{L_{\mathrm{M}}} \kappa_\ell \ T_\ell^{\mathrm{M}} \sum_{n=2}^{L} (2n+1)\lambda_n R_{\ell,n}(\psi_{\mathrm{c}}) \end{aligned} \tag{9}$$

where $R_{\ell,n}(\psi_{\mathrm{c}})$ are the Paul coefficients evaluated for the spherical cap ψ_{c} (Paul 1973)

$$R_{\ell,n}(\psi_{\mathrm{c}}) = \int_{\psi_{\mathrm{c}}}^{\pi} P_\ell(\cos\psi) P_n(\cos\psi)\sin\psi \,\mathrm{d}\psi, \quad n \le \ell \tag{10}$$

Even though all band-limited kernel functions are bounded, it is computationally advantageous to modify the near-zone contribution for the point $\psi = 0$. By adding and subtracting the gravity value $g_{\mathrm{P}}^{\mathrm{l}}$ at the singular point, the near-zone contribution can be computed as

$$f_{\sigma_0} = \frac{1}{4\pi}\iint_{\sigma_0} (g^{\mathrm{l}} - g_{\mathrm{P}}^{\mathrm{l}}) K \mathrm{d}\sigma + \frac{1}{4\pi} g_{\mathrm{P}}^{\mathrm{l}} \iint_{\sigma_0} K \mathrm{d}\sigma \tag{11}$$

$$\approx \frac{1}{4\pi}\sum_{j=1}^{N} (g_j^{\mathrm{l}} - g_{\mathrm{P}}^{\mathrm{l}}) K \Delta\Omega_j - \frac{g_{\mathrm{P}}^{\mathrm{l}}}{2}\sum_{\ell=2}^{L} (2\ell+1)\lambda_\ell R_{\ell,0}(\psi_{\mathrm{c}}) \tag{12}$$

where N is the number of data within the spherical cap and $\Delta\Omega_j$ stands for the trapezoidal cell corresponding to the jth geographical grid point. $R_{\ell,0}(\psi_{\mathrm{c}})$ is again taken from Paul (1973)

$$R_{\ell,0}(\psi_{\mathrm{c}}) = -\int_{0}^{\psi_{\mathrm{c}}} P_\ell(\cos\psi)\sin\psi \mathrm{d}\psi \tag{13}$$

$$= \frac{P_{\ell+1}(\cos\psi_{\mathrm{c}}) - P_{\ell-1}(\cos\psi_{\mathrm{c}})}{2\ell+1} \tag{14}$$

Using more than one input functional for the determination of an output functional leads to overdetermined problems. They can be solved for by introducing weighting functions $p_\ell^{(i)}$. When the weights are dependent on the degree ℓ, they are usually denoted as *spectral weights* (Sjöberg 1981). Obviously, the combination is inherently stationary. The output functional f is then determined as a weighted sum of the i different contributions

$$f_\ell = \sum_i p_\ell^{(i)} f_\ell^{(i)} \tag{15}$$

As suggested in Wenzel (1981), the weights can be incorporated into the (kernel) functions leading to a *spectral combination*. The weights are computed before the integration process and an a priori accuracy estimate of the final output functional can be obtained. For computational convenience, the common summations in the integral kernels are performed simultaneously. When f happens to be the disturbing potential at geoid level, geoidal undulations are determined using the Bruns formula.

3 The determination of the weights

Conceptually, in all combination methods such as LS collocation, multiple-input/single-output etc., the

stochastic model is the most difficult part since assumptions about the noise characteristics have to be made. However, knowledge on the noise of the terrestrial gravity anomalies is often limited, which makes the use of such a stochastic combination method rather questionable.

In the following, a quasi-deterministic (QD) solution is derived that relies on the assumption that the low-frequency information is more accurately known from satellite data and that signal degree variances from local measurements can be reliably derived. In addition, it is assumed that global and local errors are comparable in a certain frequency band. This may be achieved numerically by means of Pellinen's smoothing functions (Jekeli 1981). Theoretically, however, a comparison of global and local errors remains difficult.

3.1 Case 1

Satellite (S) and local gravity data (for instance Δg) will be combined. The spectra overlap in the low to medium frequencies since there is no satellite information above degree L_S. The original spectral combination method proposed by Wenzel (1981) and Sjöberg (1981) uses ($\forall \ell \leq L_S$)

$$p_\ell^{(1)} = 1 - p_\ell^{(2)}, \qquad p_\ell^{(2)} = \frac{\varepsilon_\ell^S}{\varepsilon_\ell^S + \varepsilon_\ell^{\Delta g}} \tag{16}$$

where ε_ℓ^S and $\varepsilon_\ell^{\Delta g}$ are the error degree variances of the satellite spherical harmonics and local anomaly data, respectively. Note that all (error) degree variances have to be in the same unit (or dimensionless) to accommodate the necessary combinations and conversions. The major objection against this stochastic model is the required knowledge of the error degree variances of the local gravity data. It is usually not available and has to be estimated.

The signal degree variances of the local data $\bar{c}_\ell^{\Delta g}$ can be written as

$$\bar{c}_\ell^{\Delta g} = c_\ell^{\Delta g} + \varepsilon_\ell^{\Delta g} \approx \; c_\ell^S + \varepsilon_\ell^{\Delta g} \tag{17}$$

where $c_\ell^{\Delta g}$ are the true (unknown) degree variances derived from the gravity anomalies and c_ℓ^S are the degree variances of the satellite spherical harmonics. Signal and noise are assumed to be uncorrelated. Solving for $\varepsilon_\ell^{\Delta g}$, Eqs. (16) and (17) yield the QD combination

$$p_\ell^{(1)} = 1 - p_\ell^{(2)}, \qquad p_\ell^{(2)} = \frac{\varepsilon_\ell^S}{\varepsilon_\ell^S + |\bar{c}_\ell^{\Delta g} - c_\ell^S|} \tag{18}$$

Taking the absolute value $|\cdots|$ ensures positive variances. Clearly, in Eqs. (18) a larger weight is assigned to the measurement type that has smaller errors, and vice versa. It is important to note that the QD combination does not require a priori knowledge of the errors in the local gravity data since $\bar{c}_\ell^{\Delta g}$ is determined from the measurements and not from observables! However, the model is not perfect since $c_\ell^{\Delta g} = c_\ell^S$ is an approximation for higher degrees and the determination of $\bar{c}_\ell^{\Delta g}$ is not error free. Nevertheless, it seems that this approximation is more reliable than other stochastic combinations because it involves weaker assumptions. For degrees $\ell > L_S + 1$, the weights are given as

$$p_\ell^{(1)} = 0, \qquad p_\ell^{(2)} = 1 \tag{19}$$

3.2 Case 2

Using three or more (independent) measurement types, the i measurement weights are determined using a Gauss–Markov model with constraints. The parameters $p_\ell^{(i)}$ are subject to the constraint

$$p_\ell^{(1)} + p_\ell^{(2)} + p_\ell^{(3)} + \cdots = 1 \tag{20}$$

The parameter vector $\mathbf{p}_\ell^T$ is then given by (Koch 1999)

$$\mathbf{p}_\ell^T = \mathbf{N}_\ell \Big\{ \mathbf{A}_\ell^T \boldsymbol{\Sigma}_\ell^{-1} \mathbf{y}_\ell + \mathbf{H}_\ell^T \left(\mathbf{H}_\ell \mathbf{N}_\ell \mathbf{H}_\ell^T \right)^{-1} \left(\mathbf{w}_\ell - \mathbf{H}_\ell \mathbf{N}_\ell \mathbf{A}_\ell^T \boldsymbol{\Sigma}_\ell^{-1} \mathbf{y}_\ell \right) \Big\} \tag{21}$$

where $\mathbf{N}_\ell = \left(\mathbf{A}_\ell^T \boldsymbol{\Sigma}_\ell^{-1} \mathbf{A}_\ell \right)^{-1}$. $\mathbf{H}_\ell$ and $\mathbf{A}_\ell$ are the coefficient matrices for the constraints and the parameters, respectively. For uncorrelated data the matrices $\mathbf{H}_\ell$, $\mathbf{A}_\ell$ and $\mathbf{w}_\ell$ are unit matrices or vectors and the vector $\mathbf{y}_\ell$ stands for the i different contributions. In Eq. (21) the covariance matrix $\boldsymbol{\Sigma}_\ell$ is given by

$\forall\ \ell = 2, \ldots, L_S$:

$$\boldsymbol{\Sigma}_\ell = \begin{pmatrix} \varepsilon_\ell^S & 0 & 0 & \\ 0 & |\bar{c}_\ell^{\Delta g} - c_\ell^S| & 0 & \\ 0 & 0 & |\bar{c}_\ell^{\delta g} - c_\ell^S| & \\ & & & \ddots \end{pmatrix} \tag{22}$$

where terms on the main diagonal are the error degree variances of the individual measurement types. Equation (22) implies that the measurement types are independent. This assumption will hold true for the new satellite missions; for some of the existing geopotential models, however, terrestrial anomalies have been used and correlations exist. For $\ell > L_S$, the covariance matrix takes the form

$\forall\ \ell = L_S + 1 \ldots L$:

$$\boldsymbol{\Sigma}_\ell = \begin{pmatrix} 0 & 0 & 0 & \\ 0 & |\bar{c}_\ell^{\Delta g} - c_\ell^{TR}| & 0 & \\ 0 & 0 & |\bar{c}_\ell^{\delta g} - c_\ell^{TR}| & \\ & & & \ddots \end{pmatrix} \tag{23}$$

In Eq. (23) it is implicitly assumed that the degree variance c_ℓ can be sufficiently approximated by the Tscherning–Rapp model degree variance c_ℓ^{TR} (Tscherning and Rapp 1974) and that the difference between them will be the same for all measurement types. It is observed that, using two or more measurement types,

the difference between a rough approximation of the gravity degree variances and the true one cancels out. Thus, the determination of the weighting functions only relies on the quality of the estimated error degree variances of the satellite missions and the determination of the signal degree variances of the local gravity data. No a priori information about the deterministic or stochastic errors in the local data is required.

The (dimensionless) degree variances of the satellite harmonics are computed as (Heiskanen and Moritz 1967)

$$c_\ell^{\mathrm{S}} = \sum_{m=0}^{\ell} (\Delta C_{\ell,m}^2 + \Delta S_{\ell,m}^2) \tag{24}$$

and the error degree variances

$$\varepsilon_\ell^{\mathrm{S}} = \sum_{m=0}^{\ell} (\delta C_{\ell,m}^2 + \delta S_{\ell,m}^2) \tag{25}$$

where $\delta C_{\ell,m}$ and $\delta S_{\ell,m}$ are the standard deviations of the fully normalized potential coefficients $\Delta C_{\ell,m}$ and $\Delta S_{\ell,m}$. The degree variances from the local data are obtained via integration (Heiskanen and Moritz 1967, p. 257)

$$\bar{c}_\ell^f = \frac{2\ell+1}{2} \lambda_\ell^2 \int_{\psi=0}^{\pi} \mathrm{COV}(\bar{g},\bar{g}) P_\ell(\cos\psi) \sin\psi \, d\psi \tag{26}$$

where $\mathrm{COV}(\bar{g},\bar{g})$ is the local empirical covariance function using noisy data $\bar{g}$. As the empirical covariance function is generally not isotropic, an averaging process over all azimuths has to be performed. λ_ℓ^2 equals 1 if the output functional f is the same as the input functional g. Due to the lack of global gravity data, the integration is limited up to a maximum ψ_{c}. Thus, the very low frequencies will not be reliably recovered by the local gravity data due to the leakage problem. Moreover, a window function as suggested by Wenzel and Arabelos (1981) should be used to avoid aliasing effects. Alternatively, the degree variances may be derived via power spectral density (PSD) functions (Schwarz et al. 1990).

4 Combination of two measurement types

In this section, numerical simulations are presented with a two-fold purpose in mind. First, the integration accuracies of two measurement-type combinations are estimated, and second, the approach proposed in this paper is compared to a deterministic combination.

The simulation parameters are summarized in Table 3. The geopotential model EGM96 (Lemoine et al. 1998) is used instead of a satellite model since a high-resolution satellite model is currently unavailable. It is combined with either gravity anomalies or airborne gravity disturbances at height H. The local gravity data are generated using a synthetic model ($L = 2160$) on a $5' \times 5'$ grid in an area of $3^\circ \times 5^\circ$. The synthetic model consists of the coefficients of the EGM96 up to degree and order 120 and a Kaula-like extension for the higher degrees [see Novák et al. (2001) for the computational details].

The gravity anomaly data range from -24.24 mGal to about $+26.71$ mGal and, thus, represent a field of medium roughness. The gravity disturbances at flight height are shown in Fig. 1. The white box indicates the output area after the integration. The geoid solution from the synthetic potential coefficients, which is assumed to be the true solution, can be directly computed on the same grid. Degrees $L_{\mathrm{S}} = 300$ and $L_{\mathrm{M}} = 360$ are used in the combination. It should be noted that $L_{\mathrm{S}} = 300$ may be an optimistic value for the GOCE mission [European Space Agency (ESA) 1999].

The weighting functions $p_\ell^{(1)}$ and $p_\ell^{(2)}$ for gravity anomalies and the geopotential model are shown in Fig. 2. They are computed using the QD approach and the EGM96 error model.

Clearly, frequencies below degree 120 cannot be resolved by local gravity data. This is mainly due to the size of the area in which the data are given. Therefore, the geopotential model receives almost full weight in the long wavelengths of the combination solution. Above degree $\ell \approx 120$, however, the signal-to-noise ratio of the geopotential model is decreasing and leads to an increasingly downweighted solution. The same weights have been chosen for airborne and terrestrial gravity data for comparison purposes. Above degree L_{S}, the weights are chosen according to Eq. (19).

The statistics for the weighted combinations are summarized in Table 4. Four combination solutions are shown. The solution on the far left is the weighted combination of noise-free gravity anomalies and EGM96. The next two columns represent the combination of noise-free airborne disturbances and EGM96. The computational steps are then repeated with noise e in the local data. White noise of 1.5 mGal standard deviation (SD) is used. These results are shown in the next two solutions; first the combination of noisy gravity anomalies with EGM96 and then noisy airborne disturbances with EGM96. Thus, the two left solutions of Table 4 demonstrate the best-case scenario whereas the two right solutions show the robustness of the combinations to noise in the local data. Common to all solu-

Table 3. Simulation parameters for two data types

Data sets		Height (m)	Error models		Results
Global	Local		Global	Local	
EGM96	δg	4000	EGM96	QD	Table 4
EGM96	Δg	0	EGM96	QD	Table 4, Fig. 2
EGM96	δg	4000	no	no	Table 5
EGM96	Δg	0	no	no	Table 5

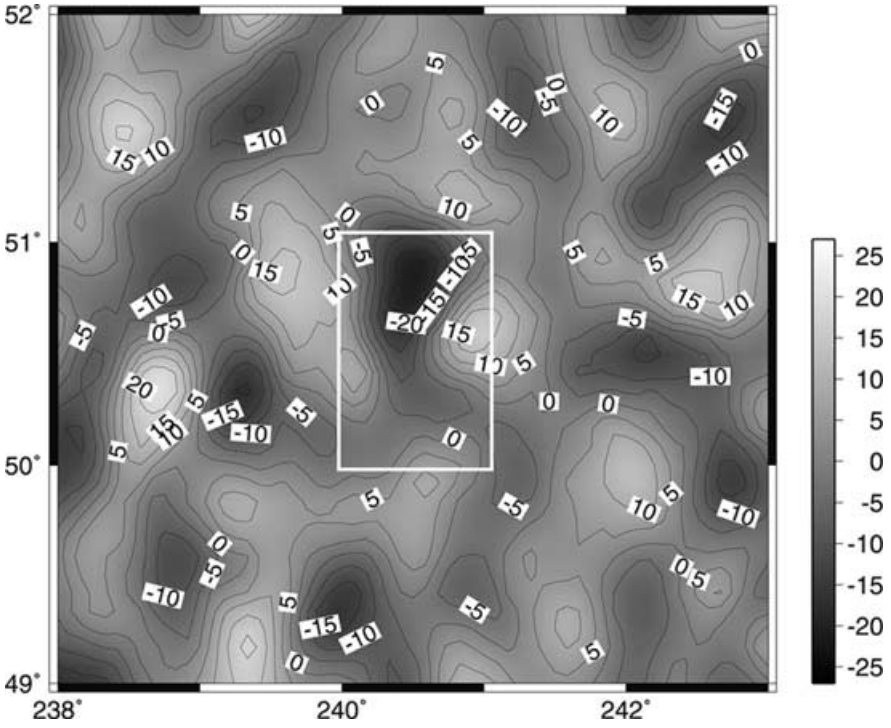

Fig. 1. Gravity disturbances at flight level (mGal)

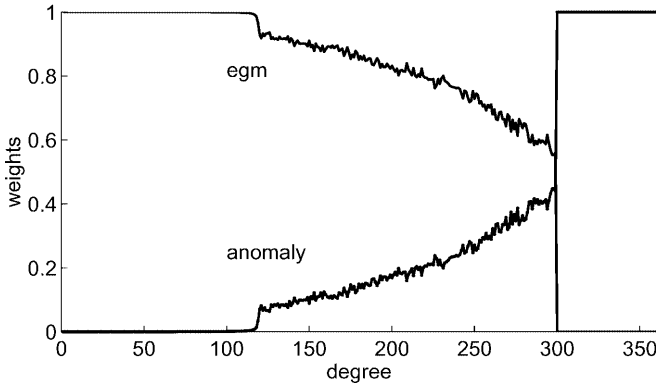

Fig. 2. Weighting functions using EGM96 and gravity anomaly data

tions is a very small far-zone contribution. This has two main reasons: first, the weights move the first zero crossings in the kernel functions slightly forward, and second, the far-zone effect from degree 301 to 360 is very small. The final geoid errors are summarized in the last row of Table 4. In all cases, the mean difference is small and the standard deviation stays within the 1–2-cm range. Thus, the chosen weight model performs reasonably well for the combination of two measurement types.

As indicated in Table 3, a deterministic combination as proposed by Vaníček and Kleusberg (1987) has also been performed. In this case, the weights in Eqs. (18) are chosen as 1 or 0 for the respective data sets, implying that the data spectra do not overlap. Obviously, the kernel function reduces to the spheroidal kernel. Additional errors are expected from such a combination and the results are shown in Table 5.

Due to the improperly modeled low to medium frequencies in the local gravity data, the mean differences are clearly larger than in the previous, weighted cases. For instance, comparing the combination errors of noisy gravity anomaly data from the deterministic and the weighted solutions, the mean differences to the true solution are 1.3 cm in the deterministic case and 0.6 cm in the weighted case. This means that the deterministic combination doubles the bias compared to the weighted solution. Thus, even though the deterministic combination is computationally easier, errors are introduced by such a procedure. Other deterministic kernel functions may be used instead (see e.g. Vaníček and Featherstone 1998).

Table 4. Geoid from weighted combination (m)

	EGM96 Δg		EGM96 δg		EGM96 $\Delta g + e$		EGM96 $\delta g + e$	
	Mean	SD	Mean	SD	Mean	SD	Mean	SD
Near zone	−0.047	0.134	−0.045	0.132	−0.047	0.135	−0.045	0.134
Far zone	+0.007	0.018	+0.007	0.017	+0.007	0.018	+0.007	0.017
Geoid	−15.582	0.180	−15.580	0.179	−15.582	0.181	−15.582	0.181
Error	+0.006	0.013	+0.005	0.012	+0.007	0.015	+0.005	0.017

Table 5. Geoid from deterministic combination (m)

	EGM96 Δg		EGM96 δg		EGM96 $\Delta g + e$		EGM96 $\delta g + e$	
	Mean	SD	Mean	SD	Mean	SD	Mean	SD
Near zone	−0.052	0.134	−0.053	0.130	−0.055	0.135	−0.053	0.133
Far zone	+0.007	0.018	+0.007	0.017	+0.007	0.018	+0.007	0.017
Geoid	−15.589	0.181	−15.588	0.181	−15.589	0.182	−15.588	0.183
Error	+0.013	0.014	+0.011	0.014	+0.011	0.015	+0.011	0.019

5 Combination of multiple measurement types

The combination of three or more measurement types on the same grid is more involved than the previously shown combinations. Prior to the combination of multiple data, datum inconsistencies and other bias-like effects are frequently removed by fitting a plane or removing a bias from the data. Airborne measurements, for instance, usually resolve a certain bandwidth extremely accurately at the cost of a possible bias (Schwarz and Li 1996). Instrumental, operational or methodological problems may lead to degradations of the low frequencies (Bruton 2000). The data can then be made consistent to other gravity information such as ground gravity anomalies through cross-over adjustments and other operations. However, this implies that the inhomogeneous ground gravity data mirror the gravity field more reliably than the airborne data. This is usually not true. Similar situations with shipborne data, altimeter data etc. exist. These rather heuristic assumptions and their solutions are unsatisfactory. The LS combination with the determination of the weights as given in Sect. 3 solves this problem and low-frequency inconsistencies in the local data do not play a major role.

The parameters for the two simulation tests are summarized in Table 6. The generated weighting functions for the three measurement types, GOCE, simulated gravity anomalies, and simulated airborne gravity disturbances, are shown in Fig. 3. The GOCE errors are predicted values for a mission duration of 12 months (ESA 1999).

The differences between the anomalies and the gravity disturbances increase at degree 250. From there on, the gravity anomalies gain more power in the combination than the disturbances. This reflects the attenuation effect for the gravity disturbances at flight height. Above degree 300, both weighting functions converge to a value of about 0.5. As in the two-measurement-type combination, the low-frequency information of the geoid stems from the satellite model. However, the weighting curve for the satellite model decreases faster due to the chosen GOCE error model and an additional measurement type.

As discussed in Wenzel (1981) and Wichiencharoen (1984), a comparison of the weighted kernel functions with their deterministic counterparts improves our understanding of the behavior of the combination. The weighted kernel functions, shown in Figs. 4 and 5, are obtained using the weighting functions for three measurement types, EGM96, gravity anomaly data, and gravity disturbances at flight level. Figure 4 shows the weighted and original Stokes kernel functions for gravity anomalies. Figure 5 in turn shows the weighted and original one-step kernel function used for the airborne data. Both figures show the kernel functions plotted versus the logarithm of the spherical distance and demonstrate that the weighted kernel functions have less power than the original kernel functions.

The first degrees in the kernel functions are virtually zero due to the chosen weights. Hence, a bias in the local gravity data does not propagate into the final solution. A cross-over adjustment for the airborne gravity disturbances, mainly removing a bias between the airborne data and the terrestrial gravity anomalies, seems therefore not to be required. This may be supported by the numerical investigation summarized in Table 7. The columns on the far left show the statistics for the combination of EGM96, noise-free gravity anomalies Δg, and gravity disturbances δg at flight height. The results with noisy data in turn are obtained when assuming white-noise characteristics of 1.5 cm SD for both local gravity data sets. An additional constant bias of 5 mGal is applied to the airborne data for the statistics summarized in the far-right columns of Table 7. Even though the local data are burdened with noise and a bias, the mean differences do not increase.

Table 6. Simulation parameters for three data types

Data sets			Error models			Results
Global	Local	Local	Global	Local	Local	
EGM96	Δg	δg	GOCE	QD	QD	Fig. 3
EGM96	Δg	δg	EGM96	QD	QD	Table 7, Figs. 4, 5, 6

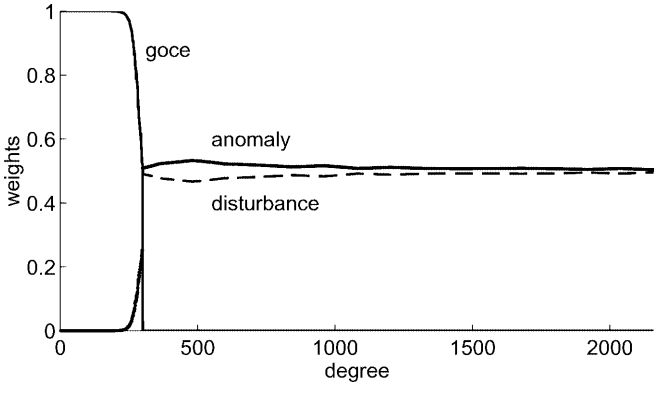

Fig. 3. Weighting functions using GOCE, gravity anomaly data and gravity disturbances

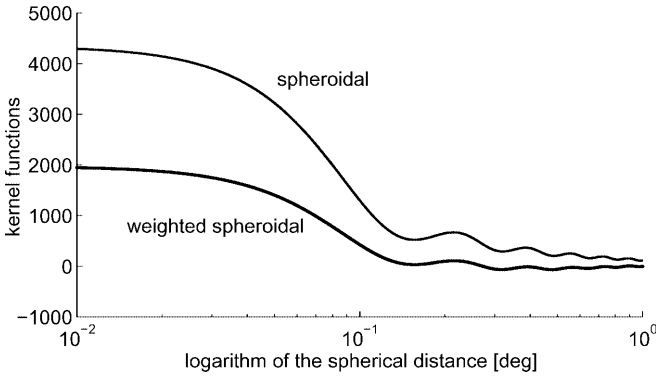

Fig. 4. Weighted spheroidal kernel versus spheroidal kernel

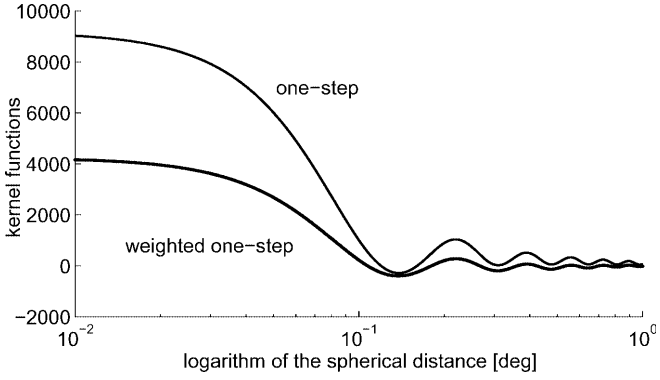

Fig. 5. Weighted one-step kernel versus one-step kernel

Table 7. Geoid from combined integration (m)

	Noise-free		Noisy		Noisy + biased	
	Mean	SD	Mean	SD	Mean	SD
Near zone	−0.048	0.132	−0.048	0.132	−0.048	0.132
Far zone	+0.004	0.009	+0.004	0.009	+0.004	0.009
Geoid	−15.586	0.180	−15.586	0.180	−15.587	0.180
Error	+0.010	0.019	+0.010	0.019	+0.010	0.019

However, the mean difference of about 1 cm is slightly larger than that for the weighted combination of two measurement types; compare Table 4. This is most likely due to the fact that integration errors are part of the combined solution.

The geoid errors represented in the last row of Table 7 are also shown in Fig. 6.

In correspondence with the statistics in the tables, only the inner $1^\circ \times 1^\circ$ part of the area is plotted in order to avoid edge effects or other numerical difficulties. Thus, Fig. 6 shows the residual errors due to integration, model, and other effects. The errors stay below the level of 2 cm.

6 Discussion and conclusions

A strategy for the combination of heterogeneous data sets has been developed. The proposed approach could be seen as a continuation of the work done by Sjöberg (1981), Wenzel (1982), and van Gelderen and Rummel (2001), and uses spectral weights for the combination. Four specific contributions and refinements are made to the original model.

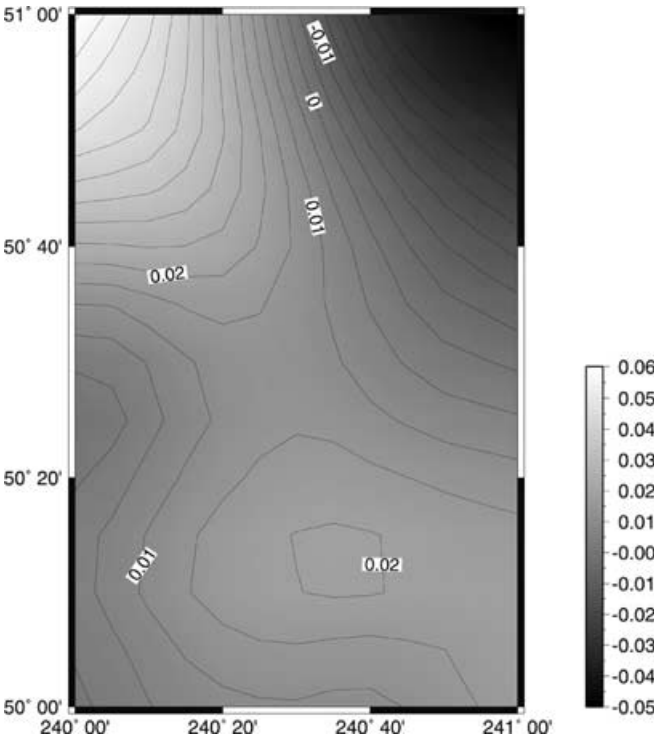

Fig. 6. Geoid error using EGM96, gravity anomalies and gravity disturbances (m)

(1) A generalization of the original spectral combination using multiple measurement types is demonstrated. Practical issues such as truncation errors and singularities are treated in a general way. Spherical approximation is used throughout the paper.
(2) A quasi-deterministic solution for the determination of the spectral weights is presented that is mainly based on the assumption that the low-frequency harmonics will be reliably known from satellite missions. When global and local (error) degree variances are considered comparable, no a priori assumptions about the noise of the local gravity data have to be made. Residual errors from gridding and correction processes are naturally included in the spectral weights. Although the noise of the local gravity data can be non-stationary, the spectral combination remains inherently stationary.
(3) A comparison to a purely deterministic two-measurement-type combination is made. Numerical results indicate that unmodeled low-frequency information in the deterministic combination propagates as a bias into the solution.
(4) In multiple measurement combinations, a bias in one of the local data sets does not propagate into the final solution. This is mainly due to the spectral weighting process. Thus, the spectral combination method represents an alternative to classical combination methods such as LS collocation.

Despite the refinements introduced, a number of questions remain. Most of them are general problems and not specific to the QD approach. They include the following.

(1) How can local and global errors be compared? How do correlations between global and local data affect the solution?
(2) Is a combination of heterogeneous gravity data significantly better on the observation level? And, how does the QD approach perform compared to traditional combination techniques such as LS collocation and multiple–input–single–output using real data?
(3) How can topographical and atmospheric reductions, biases, and other effects be treated, estimated, and included into the combination?

As can be gauged by these questions, the underlying theoretical problems still remain. This paper only provides a further step towards resolving these problems. Future theoretical studies as well as numerical investigations with real satellite, airborne, and terrestrial data will provide new insight to the problem.

Acknowledgments. Financial support has been provided by an NSERC grant of the second author. The authors wish to thank Prof. B. Heck, Dr. M. Kuhn, and Dr. P. Novák for stimulating discussions on the topic. Prof. F. Sansò and two anonymous reviewers are thanked for their thoughtful comments on an earlier version of the paper.

References

Bjerhammar A (1973) On the discrete boundary value problem in physical geodesy. Symposium on the Earth's gravitational field and its variations in position, Sidney, pp 1–13

Bruton AM (2000) Improving the accuracy and resolution of SINS/DGPS airborne gravimetry. PhD Thesis, Department of Geomatics Engineering, the University of Calgary

European Space Agency (1999) Gravity field and steady-state ocean circulation explorer. Tech rep: Reports for mission selection. The four candidate Earth core missions, ESA SP-1233(1). European Spacew Agency, Publications Division, ESTEC, Noordwijk

Featherstone WE, Evans JD, Olliver JG (1998) A Meissl-modified Vaníček and Kleusberg kernel to reduce the truncation error in gravimetric geoid computations. J Geod 72:154–160

Heck B, Grüninger W (1987) Modification of Stokes' integral formula by combining two classical approaches. In: Proc IAG Symposia on Advance in Gravity Field Modelling, XIX IUGG General Assembly, Vancouver, pp 319–337

Heiskanen WA, Moritz H (1967) Physical geodesy. WH Freeman, San Francisco

Jekeli C (1981) Alternative methods to smooth the Earth's gravity field. Tech rep 327, Department of Geodetic Science and Surveying, The Ohio State University, Columbus

Keller W (1991) Behandlung eines überbestimmten Gradiometrie-Randwertproblems mittels Pseudodifferentialoperatoren. Z Vermess 116:66–73

Koch R (1999) Parameter estimation and hypothesis testing in linear models, 2nd edn Springer, Berlin, Heidelberg, New York

Krarup T (1969) A contribution to the mathematical foundation of physical geodesy. Tech rep Meddelelse no. 44, Geodaetisk institute, Kobenhavn, Danemark

Lemoine FG, Kenyon SC, Factor JK, Trimmer RG, Pavlis NK, Chinn DS, Cox CM, Klosko SM, Luthchke SB, Torrence MH, Wang YM, Williamson R, Pavlis EC, Rapp RH, Olson TR (1998) The development of the joint NASA GSFC and NIMA geopotential model EGM96. Tech rep NASA-TP-1998-206861

Meissl P (1971) On the linearization of the geodetic boundary value problem. Tech rep 151, The Department of Geodetic Science and Surveying, Ohio State University, Columbus

Molodneskij MS (1958) Grundbegriffe der geodätischen Gravimetrie. VEB Verlag Technik, Berlin

Moritz H (1989) Advanced physical geodesy, 2nd edn. H Wichmann, Karlsruhe

Novák P, Heck B (2002) Downward continuation and geoid determination based on band-limited airborne gravity data. J. Geod. 76:269–278.

Novák P, Vaníček P, Véronneau M, Holmes SA, Featherstone WE (2001) On the accuracy of Stokes's integration in the precise high-frequency geoid determination. J Geod 74:644–654

Paul M (1973) A method of evaluation the truncation errors coefficients for geoidal heights. Bull Géod 110:413–425

Pishchukhina KV (1987) Methods for the approximation of geoid heights and deflections of the vertical. In: Holota P (ed) Proc Int Symp: Figure and Dynamics of the Earth, Moon and Plantes, Prague, pp 421–441

Rummel R, van Gelderen M (1995) Meissl scheme – spectral characteristics of physical geodesy. Manuscr Geod 20:379–385

Sacerdote F, Sansò F (1985) Overdetermined boundary value problems in physical geodesy. Manuscr Geod 10:195–207

Schwarz KP (1984) Data types and their spectral properties. In: Schwarz KP (ed) Proc Beijing International Summer School on local Gravity Field Approximation, China, pp 1–66

Schwarz KP, Li Y (1996) What can airborne gravimetry contribute to geoid determination? J Geophys Res 101(B8):17 873–17 881

Schwarz KP, Sideris MG, Forsberg R (1990) The use of FFT techniques in physical geodesy. J Geophys Res 100:485–514

Sideris MG (1996) On the use of heterogeneous noisy data in spectral gravity field modeling methods. J Geod 70:470–479

Sjöberg LE (1981) Least-squares combination of satellite and terrestrial data in physical geodesy. Ann Geophys 37:25–30

Tscherning CC, Rapp R (1974) Closed covariance expressions for gravity anomalies, geoid undulations, and deflections of the vertical implied by anomaly degree variance models. Tech Rep 208, Department of Geodetic Science, The Ohio State University, Columbus

van Gelderen M, Rummel R (2001) The solution of the general geodetic boundary value problem by least squares. J Geod 75:1–11

Vaníček P, Featherstone WE (1998) Performance of three types of Stokes's kernel in the combined solution for the geoid. J Geod 72:684–697

Vaníček P, Kleusberg A (1987) The Canadian geoid – Stokesian approach. Manuscr Geod 12:86–98

Vassiliou AA (1986) Numerical techniques for processing airborne gradiometer data. UCSE rep 20017, PhD Thesis, Department of Geomatics Engineering, The University of Calgary

Wenzel H, Arabelos D (1981) Zur Schätzung von Anomalie – Gradvarianzen aus lokalen empirischen Kovarianzfunktionen Z Vermess 5:234–243

Wenzel H-G (1981) Zur Geoidbestimmung durch Kombination von Schwereanomalien und einem Kugelfunktionsmodell mit Hilfe von Integralformeln. Z Vermess 3:102–111

Wenzel H-G (1982) Geoid computation by least-squares spectral combination using intergral kernels. In: Proceedings of the General IAG Meeting, Tokyo, pp 438–453

Wichiencharoen C (1984) A comparison of gravimetric undulations computed by the modified Molodenskij truncated method and the method of least squares spectral combination by optimal integral kernels. Bull Géod 58:494–509